Desalination and Water Treatment
www.deswater.com
doi: 10.1080/19443994.2015.1039602

57 (2016) 7918–7925
April

Taylor & Francis
Taylor & Francis Group

Removal behavior research of orthophosphate by CaFe-layered double hydroxides

Yunfeng Xu, Hetian Hou, Qiang Liu, Jianyong Liu, Li Dou, Guangren Qian*

School of Environmental and Chemical Engineering, Shanghai University, Shanghai 200444, China, Tel./Fax: +86 21 66137758; emails: yfxu@shu.edu.cn (Y. Xu), hnn2246@163.com (H. Hou), qliu@shu.edu.cn (Q. Liu), liujianyong@shu.edu.cn (J. Liu), 865112863@qq.com (L. Dou), grqian@shu.edu.cn (G. Qian)

Received 19 December 2014; Accepted 5 April 2015

ABSTRACT

The different removal behavior of orthophosphate (OP) over the CaFe-layered double hydroxides (CaFe-LDH) was investigated. The results displayed that the existence of Ca^{2+} in the solution could promote the phosphorus removal, the removal efficiency could reach 100% with 1.473 mmol P/g LDH. The kinetics fitting parameters showed that the removal process of OP was in accordance with the secondary dynamic equation, and it changed from the homogeneous reaction to heterogeneous reaction according to Elovich equation. Moreover, Freundlich isothermal adsorption equation preferably described the removal process of OP, indicated that it was a complicated process including physical and chemical adsorption. The main removal mechanism was the formation of hydroxyapatite by PO_4^{3-} and Ca^{2+} dissolved from LDHs, and ferrihydrite could also strengthen the OP removal effect via the formation of surface complexes.

Keywords: CaFe-LDH; Orthophosphate; Removal; Adsorption

1. Introduction

Due to the extensive application in a wide range of industrial and agricultural activities, such as synthetic detergents, pesticide, and fertilizer, excess discharge of phosphorus into rivers and lakes caused water body eutrophication [1,2], which arouse wide concern for water quality and human health. Phosphate was commonly found in sewage in the forms of orthophosphate (OP) ($H_2PO_4^-$, HPO_4^{2-}, and PO_4^{3-}), polyphosphates ($P_2O_7^{4-}$, $P_3O_{10}^{5-}$, and $(PO_3)_n^{n-}$), and metaphosphate (phospholipids, etc.) [3]. As the main existence of OP (more than 50% of total phosphorus) in sewage, OP removal has been paid great attention for many years, especially OP removal techniques [4,5].

Among many techniques, chemical coagulation/precipitation has been regarded as the most effective method and has attracted much attention. Relevant researches focused on the choice and preparation of efficient adsorbent, or the behavior and influencing factors of phosphorus adsorption. The common adsorbent mainly included metal salts, oxide and hydroxide of calcium, aluminum, iron, and magnesium [6–8]. Some industrial wastes or by-products (such as

*Corresponding author.

Presented at the 7th International Conference on Challenges in Environmental Science and Engineering (CESE 2014) 12–16 October 2014, Johor Bahru, Malaysia

alum sludge [9], fly ash [10], furnace slag [11], and red mud [12].) were also utilized as cheaper adsorbent for OP removal, but always accompanied with the complex reaction process. As a result, it was desirable to find more efficient material for OP removal.

Layered double hydroxide (LDH) was a novel adsorbent with layered structure which had strong adsorption ability, anions exchange property, and higher exchange capacity [13]. So the structural features of LDH were conducive to OP removal, especially to severe OP-contaminated water fields. Badreddine et al. [14] had confirmed the ion exchange between different phosphate ions ($H_2PO_4^-$, HPO_4^{2-}, and PO_4^{3-}, etc.) and chloride of the as-prepared ZnAl–Cl–LDH. Compared the adsorption capabilities of various LDHs with different metal hydroxide layers, Ca-based LDH seemed to be significant in shorter reaction time, and the metal phosphate product was more stable in thermodynamics [15]. Radha et al. [16] revealed that there was a two-step process in the anion exchange reactions of Ca-based LDH, and its mechanism was known as the dissolution–reprecipitation. Some researchers had proved that intercalation and precipitation were the main ways of Ca-based LDH to remove dissolved anion effectively, one way was intercalation of anion into the interlayer spacing, and the other was the precipitation of dissolved Ca^{2+} with anion [17–19]. Additionally, Seida and Nakano [20] found that Fe-based LDH also expressed better effect for phosphate fixation through coagulants by the released cations and/or hydroxides. Specially, the removal efficiency was largely increased with larger buffering capacity.

CaFe-LDH was a kind of Ca-based LDH and could be simply synthesized. Sipiczki et al. [21] had formed CaFe-LDH in a co-precipitation method and studied the effect of Ca(II)/Fe(III) ratios on the stability of LDH. CaFe-LDH had been utilized to remove pyrophosphate with a maximum removal capacity of 4.54 mmol P/g LDH within 24 h [22]. In addition, CaFe-LDH revealed a higher removal amount of triphosphate (1.82 mmol P/g LDH) compared with MgFe-LDH in our previous work [23]. So CaFe-LDH was utilized to treat OP polluted wastewater based on the superiority of LDH in phosphate removal.

Herein, the current study was purposed to (1) investigate the dissolution characteristic of CaFe-LDH; (2) explore the removal behavior of OP on synthesized CaFe-LDH; (3) analyze solution component and solid products after the reaction; (4) identify the OP removal mechanism over CaFe-LDH according to adsorption kinetic and isothermal adsorption experiment. Four adsorption kinetic equations and two isotherms adsorption equations would be used to simulate the adsorption data of OP.

2. Materials and methods

2.1. Synthesis and hydrolysis of CaFe-LDH

CaFe-LDH was prepared by coprecipitation method reported elsewhere [21]. The hydrolysis was performed in a 250 mL plastic bottle with 100 mL double-distilled water (pH 11.0, adjusted by nitric acid and sodium hydroxide in advance), and 0.1 g CaFe-LDH. The bottle was placed at 25 ± 1°C in a shaking water bath. Sampling was carried out at 1, 5, 10, 20, 30 min, 1, 1.5, 2, 4, 6, 8, 12, 24, 36, and 48 h, respectively. The solution samples were filtrated for further determination of Ca^{2+} and Fe^{3+} concentration.

2.2. Removal of OP by CaFe-LDH

The effect of time on OP removal was recorded at the initial OP concentration ([OP]) of 1.473, 3.235, 5.339, 6.542, and 8.248 mmol/L. The removal reaction was performed in a beaker with 1.0 g CaFe-LDH and 1,000 mL sodium phosphate solution of five concentrations. Nitric acid and sodium hydroxide were used to adjust pH to 11.0. The mixed solution was put on a magnetic stirrer at room temperature. Fifteen sampling time points were same as those in 2.1. Then these samples should be filtered with 0.45 μm filtration membrane and stored for measurement of pH and [OP].

The isotherm of OP removal was carried out in 250 mL plastic bottle with 0.1 g CaFe-LDH and 100 mL OP solution with various initial [OP], ranging from 2.58 to 8.39 mmol/L, and the initial pH was adjusted to 11.0. After 48 h stirring by a magnetic stirrer at room temperature, samples should be filtered with 0.45 micron filtration membrane to determinate the pH, [OP], Ca^{2+}, and Fe^{3+} concentration. And the solid product was drying at 70°C in a vacuum oven for further analysis.

2.3. Analysis and characterization methods

An Elico digital pH meter (PHS-3C) was acquired to measure the pH value with a combined glass electrode (E-201-C). The OP concentration was determined by the ion chromatographic method. The ion chromatograph (ICS-1100, Diane Co.), was equipped with a reagent-free controllers (RFC-30) for eluent generation, which could provide the eluent concentration in the range of 0.1–100 mM, at a flow rate from 0.01 to

3.00 mL/min with a maximum operating pressure of 21 MPa. The concentrations of Ca^{2+} and Fe^{3+} were detected by inductively coupled plasma-atom emission spectrometer (ICP-AES, Prodidy, Leeman Co.).

Adopting a D\MAX-2200 X-ray diffractometer (Rigaku Co.) to monitor the solid product, with Cu Kα radiation and λ of 1.5406 Å at 40 kV and 100 mA. The scanning rate was set to 8°/min from 5° to 80° (2θ). The solid sample was mixed and grinded with KBr to make preforming, which was further characterized with the FTIR spectrum (Thermo, Scientific 380 FTIR) in the range of 4,000–400 cm^{-1} with resolution of 4 cm^{-1}.

3. Results and discussion

3.1. Dissolution characteristics of CaFe-LDH

The XRD pattern and FTIR spectrum of synthesized CaFe-LDH had been reported in our previous work [22]. Its structure was similar to hydrocalumite with three typical planes of (0 0 3), (0 0 6), and (1 1 0) [24,25]. A weak diffraction peak at 2θ of 29.4° identified the existence of $CaCO_3$, which might be caused by little dissolution of CO_2 from air during the synthetic process.

The strong band at 3,585 cm^{-1} referred to lattice water molecules and the O–H stretching vibration (v_{O-H}). The band near 1,620 cm^{-1} was assigned to δ_{H-O-H}. In addition, two bands at 742 and 575 cm^{-1} were observed to be the M–O vibrations, in which M is referred to Ca or Fe. Also the stretching vibration of CO_3^{2-} at 1,480 cm^{-1} indicated CO_2 dissolution during the synthesis process of CaFe-LDH, which was consistent with the XRD pattern.

Actually, the synthetic CaFe-LDH would partially dissolve in water. In the pre-test, 0.1 g CaFe-LDH was mixed with 100 mL redistilled water. After 48 h, leaching amount of Fe^{3+} was below detection limit, indicated the stable existence of Fe element in the layer structure. Conversely, Ca^{2+} released rapidly, as shown in Fig. 1. Concentration of Ca^{2+} increased dramatically within the first 2 h and reached equilibrium after 8 h. The dissolution quantity of equilibrium was about 230 mg Ca/g LDH. According to some previous studies [26,27], the existence of Ca^{2+} in the solution could promote the phosphorus removal in the wastewater treatment. The influence of dissolved Ca^{2+} on OP removal had been considered in the following research.

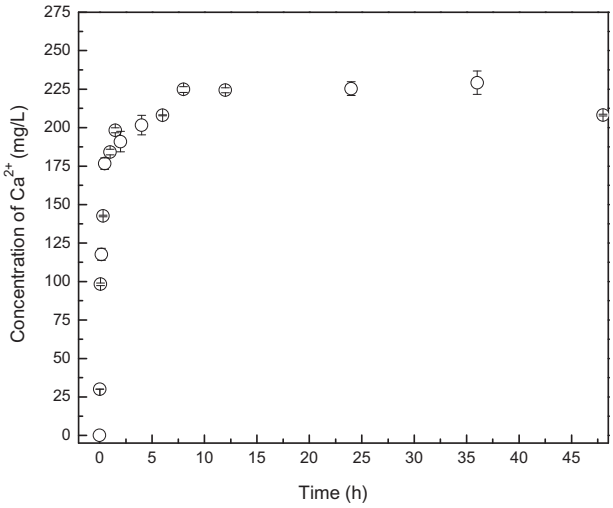

Fig. 1. Release of Ca^{2+} in the process of CaFe-LDH dissolution.

3.2. Removal of OP on CaFe-LDH

3.2.1. Effect of reaction time

The effect of reaction time on the removal of OP over CaFe-LDH is presented in Fig. 2. The variation trend of [OP] was similar for different initial concentrations with the increase in reaction time. The [OP] declined fast at the beginning of the reaction, and then flattened out until equilibrium was reached. The residual concentrations of OP were below detection limit, 0.4229, 1.911, 3.089, and 4.625 mmol P/L, respectively. The adsorption capacity of CaFe-LDH for OP increased with the extension of time, and gradually achieved equilibrium. The absorptive capacity was 1.473, 2.812, 3.428, 3.453, and 3.623 mmol P/g, respectively. The adsorption equilibrium times were about 5, 24, 32, 36, and 40 h, respectively. Compared to higher

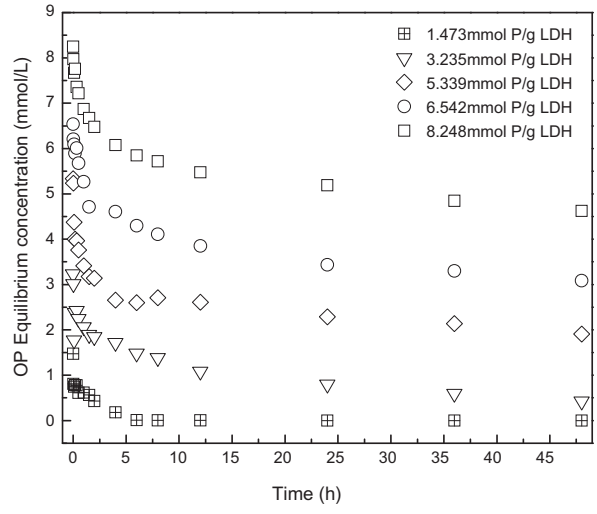

Fig. 2. The effect of reaction time on the removal of OP by CaFe-LDH.

concentration, the adsorption reaction was able to achieve a balance in a short time under lower concentration. It was obvious that the reaction rate of OP removal by CaFe-LDH was reduced with the increased [OP]. From the perspective of adsorption dynamics, the initial adsorption rate of CaFe-LDH was considerably larger than desorption rate. Afterward, the desorption rate gradually increased. Until the adsorption and desorption rate were equal, the reaction reached equilibrium.

In all tests, the removal efficiencies were 100% (1.473 mmol P/g LDH), 86% (3.235 mmol P/g LDH), 64% (5.339 mmol P/g LDH), 52% (6.542 mmol P/g LDH), and 43% (8.248 mmol P/g LDH) after equilibrium. It was evident that the increase in [OP] could affect removal efficiency and extend the time of reaching equilibrium.

3.2.2. Adsorption kinetic

The adsorption data of OP were simulated by pseudo-first-order kinetic, pseudo-second-order kinetic, intraparticle diffusion model, and Elovich equation, as expressed in the following Eqs. (1)–(4):

$$q_t = q_{e1}[1 - \exp(-kt)] \tag{1}$$

$$q_t = k_2 {q_{e2}}^2 t/(1 + k_2 q_e t) \tag{2}$$

$$q_t = K_p t^{1/2} + C \tag{3}$$

$$q_t = \frac{1}{\beta}\ln\left(\frac{\alpha}{\beta}\right) + \frac{1}{\beta}\ln t \tag{4}$$

where t (h) refers to the reaction time, and q_t (mmol/g) is the adsorption amounts at time t. q_{e1} (mmol/g), and q_{e2} (mmol/g) represent equilibrium absorption capacity of first-order and second-order adsorption, respectively. k_1 (1/h) and k_2 (g/mmol/h) refer to the rate constant of first-order and second-order adsorption. C and K_p (mmol/g/h$^{1/2}$) are the intercept and rate constant of intraparticle diffusion equation. α (mmol/g/h) and $\frac{1}{\beta}$ (g/mmol) respectively represent initial adsorption rate and desorption constant of Elovich equation.

As listed in Table 1, the model simulation was carried out with five initial [OP] conditions. According to the higher correlation coefficient (R^2), pseudo-second-order kinetic model fitted better than the other models with the experimental data at higher initial concentrations, but R^2 values were small at lower concentrations (1.473 and 3.235 mmol P/g LDH). It indicated that the mechanism of CaFe-LDH for OP removal was complicated, including surface adsorption, and the precipitation of PO_4^{3-} and Ca^{2+} dissolved from LDHs. So it could not simply be described by pseudo-second-order or pseudo-first-order kinetic equation. Additionally, R^2 of Elovich equation became larger at higher concentrations, demonstrated the homogeneous reaction converted to heterogeneous reaction.

As the rate constant (k_2) of pseudo-second-order kinetic model decreased with the increase in [OP], the reaction needs longer time to achieve equilibrium. This was consistent with the result, as shown in Fig. 2. Furthermore, the initial adsorption rate α of Elovich equation had a significant decrease as the [OP] increased, corresponding to the longer equilibrium time.

3.3. Isothermal adsorption

3.3.1. Analysis of solution component

The adsorption isotherm of OP is illustrated in Fig. 3. It could be figured out that the adsorption amount gradually increased from low concentrations to high ones and became stable from 4.0 mmol/g. The removal efficiency of different initial [OP] was 99.82, 95.73, 88.04, 77.92, 67.79, 60.28, 54.30, 51.71, 46.51, and 43.68%.

As the original pH was 11.0, the solution pH values were all ranged from 12 to 12.3 after the reaction reaching equilibrium, which suggested the dissolution of CaFe-LDH. When [OP] varied from 2.22 to 3.05 mmol/g, the concentration of Ca^{2+} decreased from 0.152 mmol/L to 0, hydroxyapatite was formed by precipitation of Ca and OP. According to theoretical calculations (Ca/p = 5/3 in the precipitation), information of hydroxyapatite needed 0.152 mmol of Ca^{2+} and 0.09 mmol PO_4^{3-} (per gram LDH). However, the increment of practical adsorption amount was about 0.70 mmol P/g, which was much greater than theoretical value. Thus, there must be other OP-fixation functions of CaFe-LDH. Besides, the concentrations of Fe^{3+} in the solution were always close to zero after reaction. It could be assumed that there was no formation of $FePO_4$.

The isotherms data were simulated by Langmuir and Freundlich models. Eqs. (5) and (6) were listed as follows:

$$Q_e = Q_m b C_e/(1 + bC_e) \tag{5}$$

$$Q_e = K_f {C_e}^{1/n} \tag{6}$$

Table 1
The adsorption kinetic parameters of OP on CaFe-Cl-LDHs

Equation		Concentration (mmol P/g LDH)				
		1.473	3.235	5.339	6.542	8.248
Pseudo-first-order equation	k_1 (1/h)	2.77	0.831	1.71	0.511	0.490
	q_{e1} (mmol/g)	1.31	2.16	2.79	2.87	2.99
	R^2	0.2600	0.4584	0.8177	0.8775	0.8793
Pseudo-second-order equation	k_2 (g/mmol/h)	4.37	1.24	2.60	0.616	0.637
	q_{e2} (mmol/g)	1.39	2.34	2.97	3.22	3.31
	R^2	0.5096	0.6070	0.9147	0.9436	0.9464
Elovich equation	α (mmol/g/h)	3.97×10^2	13.87	10.20	2.22	2.26
	$\frac{1}{\beta}$ (g/mmol)	4.25	8.90	12.18	13.74	14.14
	R^2	0.8461	0.8371	0.9814	0.9323	0.9536
Intraparticle diffusion equation	K_p (mmol/g/h$^{1/2}$)	4.20	9.76	11.35	14.56	14.77
	C	24.64	26.02	40.31	21.22	23.93
	R^2	0.6902	0.8627	0.7080	0.8778	0.8828

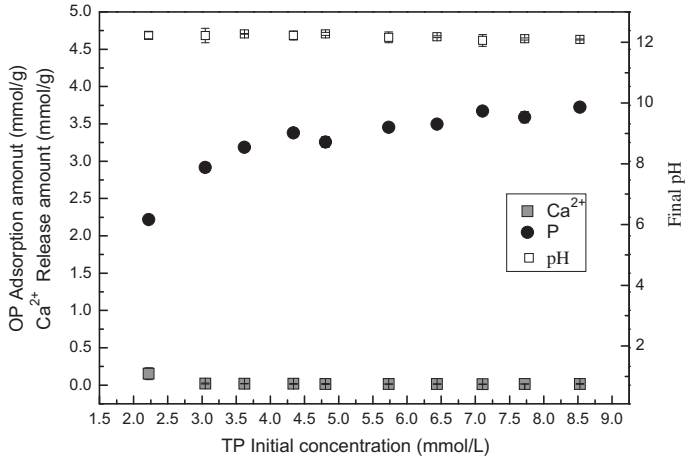

Fig. 3. Adsorption isotherm of OP on CaFe-LDH.

where Q_e and Q_m (mmol/g) refer to the equilibrium adsorption capacity and the maximum loading corresponding to complete coverage of the surface by solutes. C_e (mmol/L) presents the equilibrium concentration. b (L/mmol) is Langmuir coefficient. K_f and n are Freundlich constants.

According to the correlation coefficient (R^2) values in Table 2, Freundlich isotherms equation was well fitted with the experimental results than Langmuir, with good correlation coefficient ($R^2 = 0.93$), which could better describe the removal process of OP, and Freundlich characteristic constant ($1/n$) was 0.07. However, it was conducive to adsorb when $1/n$ was between 0.1 and 0.5. This indicated that adsorption was not the main removal performance. Combined with solution components analysis in Fig. 3, it was concluded that the removal reaction was a complicated process including chemical adsorption and precipitation, and the main reaction was precipitation of Ca^{2+} and PO_4^{3-}.

Table 2
The adsorption isotherm parameters of OP on CaFe-LDH

Freundlich			Langmuir		
$1/n$	K_f	R^2	Q_m	b	R^2
0.07	3.27	0.93	3.38	457.8	0.73

3.3.2. Characterization of solid products

The XRD patterns of the synthesized LDH and solid products are depicted in Fig. 4. The pattern for hydroxyapatite ($Ca_{10}(PO_4)_6(OH)_2$ (PDF #09-0432)) was identified predominantly in three solid products with characteristic peak at 2θ from 20˚ to 40˚. With the increase in initial [OP] (from 2.581 to 7.712 mmol P/g LDH), the characteristic peak was enhanced more obviously, illustrated that the formation of crystalline $Ca_{10}(PO_4)_6(OH)_2$ depended on initial [OP] and supported by precipitation of Ca^{2+} and PO_4^{3-} ions dispersed in the solution.

The broad peak at 2θ from 30˚ to 40˚ and 60˚ to 65˚ in three solid products indicated that the amorphous ferrihydrite ($Fe_5O_7(OH)\cdot 4H_2O$, PDF 29-0712) was present [28,29]. Because the characteristic peak of ferrihydrite weakened with the increase in [OP], it could be speculated that there was complexation between OP and ferrihydrite on the surface, which had also been mentioned in other research [30]. It was supposed to be another pathway for OP removal by CaFe-LDH besides the chemical precipitation of Ca^{2+}.

The mineral phase of products after the removal of OP was further confirmed by the FTIR spectrum in Fig. 5. New absorption peaks appeared at 1,054, 604, and 560 cm^{-1} when the initial [OP] was 2.581 mmol P/g LDH (0.1 g CaFe-LDH was added to 100 mL OP solution with the concentration of 80 mg P/L). Compared with previous studies [31,32], it could be seen that the band in the range of 1,010–1,110 cm^{-1} represented the $v3$ vibration of PO_4^{3-}, and the bands at the range of 560–610 cm^{-1} referred to the $v4$ and $v1$ vibration of PO_4^{3-} in $Ca_{10}(PO_4)_6(OH)_2$. These results were consistent with the XRD pattern, proved the main removal path was the precipitation of PO_4^{3-} and Ca^{2+} with the formation of hydroxyapatite.

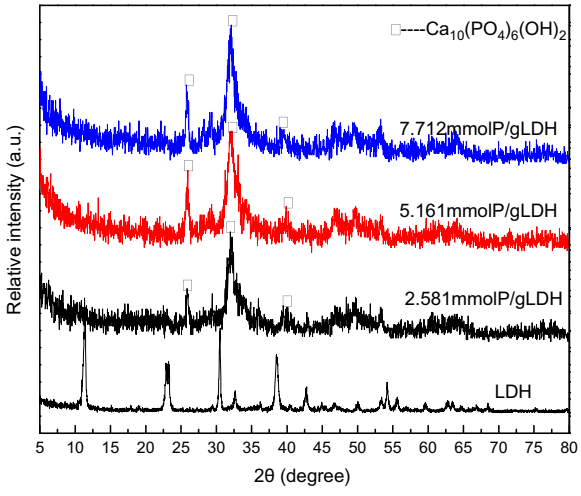

Fig. 4. XRD pattern of products after OP removal on CaFe-LDH at different initial concentrations.

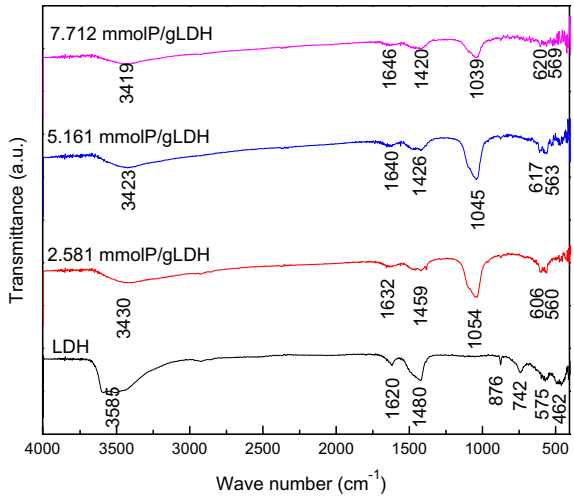

Fig. 5. FTIR spectra of the products after OP removal on CaFe-LDH at different initial concentrations.

Compared with the FTIR spectrum of synthesized CaFe-LDH, it could be seen from the FTIR spectrum of solid production that the characteristic vibration (v_{O-H}) of the constitutional water in CaFe-LDH shifted from 3,585 cm^{-1} to smaller wave band, which was closer to the band of oxhydryl in ferrihydrite [33]. It might indicate more production of Fe–O–H during the removal process of OP by CaFe-LDH. Moreover, the peak of ferrihydrite in the product was weaker than LDH, declared that Fe participated in the removal of OP in the form of ferrihydrite via surface complexing with phosphate, which strengthened the removal effect [34,35].

4. Conclusions

In this work, the different removal behavior of OP over the CaFe-LDH was investigated. More dissolution of Ca^{2+} in the solution promoted the phosphorus removal, and the increase in [OP] affected removal efficiency and extend the time of reaching equilibrium. The kinetics fitting parameters showed that the pseudo-second-order kinetic model gets better agreement with the removal process of OP. According to Elovich equation, the reaction changed from the homogeneous to heterogeneous at the higher concentrations. Furthermore, Freundlich isotherms equation preferably described the removal process of OP, which indicated that the reaction was a complicated process including chemical adsorption and precipitation. The

main removal mechanism was the precipitation between PO_4^{3-} and Ca^{2+} dissolved from LDHs with the formation of hydroxyapatite. And Fe participated in the removal of OP in the form of ferrihydrite via surface complexing with OP, which strengthened the removal effect.

Acknowledgments

This project is financially supported by the National Nature Science Foundation of China (No. 21107067/B070303, No. 41472312/D0218) and Innovative Research Team in University (No. IRT13078).

References

[1] X. Xu, B. Gao, W. Wang, Q. Yue, Y. Wang, S. Ni, Adsorption of phosphate from aqueous solutions onto modified wheat residue: Characteristics, kinetic and column studies, Colloids Surf., B 70 (2009) 46–52.
[2] H. Yin, Y. Yun, Y. Zhang, C. Fan, Phosphate removal from wastewaters by a naturally occurring, calcium-rich sepiolite, J. Hazard. Mater. 198 (2011) 362–369.
[3] L. Zeng, X. Li, J. Liu, Adsorptive removal of phosphate from aqueous solutions using iron oxide tailings, Water Res. 38 (2004) 1318–1326.
[4] L. Lin, C. Wan, D. Lee, Z. Lei, X. Liu, Ammonium assists orthophosphate removal from high-strength wastewaters by natural zeolite, Sep. Purif. Technol. 133 (2014) 351–356.
[5] C. Warwick, A. Guerreiro, A. Soares, Sensing and analysis of soluble phosphates in environmental samples: A review, Biosens. Bioelectron. 41 (2013) 1–11.
[6] X.-H. Guan, G.-H. Chen, C. Shang, Adsorption behavior of condensed phosphate on aluminum hydroxide, J. Environ. Sci. 19 (2007) 312–318.
[7] J. Zhou, S. Yang, J. Yu, Facile fabrication of mesoporous MgO microspheres and their enhanced adsorption performance for phosphate from aqueous solutions, Colloids Surf., A 379 (2011) 102–108.
[8] R. Chitrakar, A. Sonoda, Y. Makita, T. Hirotsu, Selective uptake of phosphate ions from sea water on inorganic ion-exchange materials, in: J.A. Daniels (Ed.), Advances in Environmental Research, Nova Science Publishers Inc, New York, NY, 2011, pp. 119–152.
[9] Y. Yang, Y. Zhao, P. Kearney, Influence of ageing on the structure and phosphate adsorption capacity of dewatered alum sludge, Chem. Eng. J. 145 (2008) 276–284.
[10] E. Yildiz, Phosphate removal from water by fly ash using crossflow microfiltration, Sep. Purif. Technol. 35 (2004) 241–252.
[11] Y. Yang, Y. Zhao, A. Babatunde, L. Wang, Y. Ren, Y. Han, Characteristics and mechanisms of phosphate adsorption on dewatered alum sludge, Sep. Purif. Technol. 51 (2006) 193–200.
[12] Y. Zhao, L. Zhang, F. Ni, B. Xi, X. Xia, X. Peng, Z. Luan, Evaluation of a novel composite inorganic coagulant prepared by red mud for phosphate removal, Desalination 273 (2011) 414–420.
[13] A. Halajnia, S. Oustan, N. Najafi, A.R. Khataee, A. Lakzian, Adsorption–desorption characteristics of nitrate, phosphate and sulfate on Mg–Al layered double hydroxide, Appl. Clay Sci. 80–81 (2013) 305–312.
[14] M. Badreddine, A. Legrouri, A. Barroug, A. De Roy, J.P. Besse, Ion exchange of different phosphate ions into the zinc–aluminium–chloride layered double hydroxide, Mater. Lett. 38 (1999) 391–395.
[15] Y.F. Xu, Y. Dai, J. Zhou, Z.P. Xu, G. Qian, G.M. Lu, Removal efficiency of arsenate and phosphate from aqueous solution using layered double hydroxide materials: Intercalation vs. precipitation, J. Mater. Chem. 20 (2010) 4684–4691.
[16] A. Radha, P. Vishnu Kamath, C. Shivakumara, Mechanism of the anion exchange reactions of the layered double hydroxides (LDHs) of Ca and Mg with Al, Solid State Sci. 7 (2005) 1180–1187.
[17] K. Grover, S. Komarneni, H. Katsuki, Synthetic hydrotalcite-type and hydrocalumite-type layered double hydroxides for arsenate uptake, Appl. Clay Sci. 48 (2010) 631–637.
[18] Q. Guo, J. Tian, Removal of fluoride and arsenate from aqueous solution by hydrocalumite via precipitation and anion exchange, Chem. Eng. J. 231 (2013) 121–131.
[19] Y. Li, J. Wang, Z. Li, Q. Liu, J. Liu, L. Liu, X. Zhang, J. Yu, Ultrasound assisted synthesis of Ca–Al hydrotalcite for U(VI) and Cr(VI) adsorption, Chem. Eng. J. 218 (2013) 295–302.
[20] Y. Seida, Y. Nakano, Removal of phosphate by layered double hydroxides containing iron, Water Res. 36 (2002) 1306–1312.
[21] M. Sipiczki, E. Kuzmann, Z. Homonnay, The structure and stability of CaFe layered double hydroxides with various Ca: Fe ratios studied by Mössbauer spectroscopy, X-ray diffractometry and microscopic analysis, J. Mol. Struct. 2013 (1044) 116–120.
[22] Y. Wu, Y. Yu, J.Z. Zhou, J. Liu, Y. Chi, Z.P. Xu, G. Qian, Effective removal of pyrophosphate by Ca–Fe–LDH and its mechanism, Chem. Eng. J. 179 (2012) 72–79.
[23] J. Zhou, Z. Xu, S. Qiao, Enhanced removal of triphosphate by MgCaFe-Cl-LDH: Synergism of precipitation with intercalation and surface uptake, J. Hazard. Mater. 189 (2011) 586–594.
[24] F. Millange, R.I. Walton, L. Lei, D. O'Hare, Efficient separation of terephthalate and phthalate anions by selective ion-exchange intercalation in the layered double hydroxide $Ca_2Al(OH)_6{\cdot}NO_3{\cdot}2H_2O$, Chem. Mater. 12 (2000) 1990–1994.
[25] Y. Wu, Y. Chi, H. Bai, G. Qian, Y. Cao, J. Zhou, Y. Xu, Q. Liu, Z.P. Xu, S. Qiao, Effective removal of selenate from aqueous solutions by the Friedel phase, J. Hazard. Mater. 176 (2010) 193–198.
[26] W. Li, J. Zhou, J. Zhang, J. Zhao, Y. Xu, G. Qian, pH-Dependent improvement of pyrophosphate removal on amorphous ferric hydroxide by incorporating Ca^{2+}, Chem. Eng. J. 225 (2013) 372–377.
[27] T. Vasudevan, P. Somasundaran, C. Howie-Meyers, D. Elliott, K. Ananthapadmanabhan, Interaction of pyrophosphate with calcium phosphates, Langmuir 10 (1994) 320–325.
[28] E.M. Moon, C.L. Peacock, Adsorption of Cu(II) to ferrihydrite and ferrihydrite–bacteria composites:

Importance of the carboxyl group for Cu mobility in natural environments, Geochim. Cosmochim. 92 (2012) 203–219.
[29] P. Refait, M. Reffass, J. Landoulsi, R. Sabot, M. Jeannin, Role of phosphate species during the formation and transformation of the Fe(II–III) hydroxycarbonate green rust, Colloids Surf., A 299 (2007) 29–37.
[30] N. Khare, J.D. Martin, D. Hesterberg, Phosphate bonding configuration on ferrihydrite based on molecular orbital calculations and XANES fingerprinting, Geochim. Cosmochim. Acta 71 (2007) 4405–4415.
[31] S. Ng, J. Guo, J. Ma, S.C.J. Loo, Synthesis of high surface area mesostructured calcium phosphate particles, Acta biomater. 6 (2010) 3772–3781.
[32] F. Wang, M.-S. Li, Y.-P. Lu, Y.-X. Qi, Y.-X. Liu, Synthesis and microstructure of hydroxyapatite nanofibers synthesized at 37˚C, Mater. Chem. Phys. 95 (2006) 145–149.
[33] Y. Jia, L. Xu, X. Wang, G. Demopoulos, Infrared spectroscopic and X-ray diffraction characterization of the nature of adsorbed arsenate on ferrihydrite, Geochim. Cosmochim. Acta 71 (2007) 1643–1654.
[34] P.A. Connor, A.J. McQuillan, Phosphate adsorption onto TiO_2 from aqueous solutions: An *in situ* internal reflection infrared spectroscopic study, Langmuir 15 (1999) 2916–2921.
[35] J.L. Jambor, J.E. Dutrizac, Occurrence and constitution of natural and synthetic ferrihydrite, a widespread iron oxyhydroxide, Chem. Rev. 98 (1998) 2549–2586.